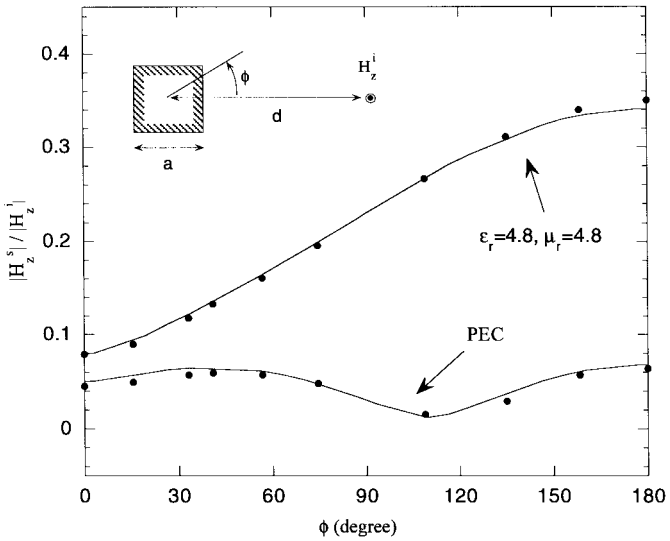

Fig. 2. Amplitude of the scattered magnetic field normalized with respect to the incident field, computed by using the subgridded mesh (···), and a fully FDTD scheme (—).

TABLE I
RESONANT FREQUENCIES (GHz) OF THE FIRST FOUR MODES OF A PARTIALLY FILLED RECTANGULAR CAVITY

Analytical	FE/FDTD	FDTD
0.782	0.782	0.782
	1.521	1.523
1.609	1.603	1.607
1.757	1.751	1.759

REFERENCES

[1] M. Okoniewski, E. Okoniewska, and M. A. Stuchly, "Three-dimensional subgridding algorithm for FDTD," *IEEE Trans. Antennas Propagat.*, vol. 45, pp. 422–429, Mar. 1997.

[2] M. W. Chevalier, R. J. Luebbers, and V. P. Cable, "FDTD local grid with material transverse," *IEEE Trans. Antennas Propagat.*, vol. 45, pp. 411–421, Mar. 1997.

[3] A. Monorchio and R. Mittra, "A hybrid finite element/finite-difference time-domain (FE/FDTD) technique for solving complex electromagnetic problems," *IEEE Microwave Guided Wave Lett.*, vol. 8, pp. 93–95, Feb. 1998.

An Adaptive-Window-Width Short-Time Fourier Transform for Visualization of Radar Target Substructure Resonances

E. J. Rothwell, K. M. Chen, and D. P. Nyquist

***Abstract*— A short-time Fourier transform with an adaptive window width is used to analyze the transient response of radar targets. The described algorithm allows the isolation and identification of substructure resonances as well as localized specular reflections and slowly building global resonances.**

***Index Terms*—Fourier transforms, radar target recognition, transient scattering.**

I. INTRODUCTION

The use of time-frequency (T-F) analysis to provide a visual aid for the understanding of complicated temporal events has a long history in science. Ornithologists have for decades employed mechanically-recorded "spectrograms" to unravel the harmonically rich reverberations of bird song [1]. Recently, electromagnetics researchers have begun using T-F analysis as a visual tool in the study of transient EM problems, often employing the short-time Fourier transform (STFT) or the wavelet transform to provide multiresolutional information [2]–[6]. This letter describes the use of a STFT with an adaptive window width for identifying substructure resonances in the transient scattered-field responses of radar targets.

II. PHENOMENOLOGICAL DISCUSSION

When a short EM pulse interacts with a radar target, the back-scattered field waveform contains a variety of temporal events, corresponding to both local and global properties of the target. Specular events are returned from surfaces and edges aligned with the scattering direction, and longer duration resonance phenomena are initiated through induced travelling-wave currents. If the duration of the incident pulse is small enough to resolve target substructures, then the scattered field waveform is a complicated jumble of specular reflections and dying and building substructure resonances, against the background of slowly established global resonances. Often the substructure resonances have decayed to zero long before the global resonances are completely formed.

Because of the complicated nature of the transient scattered field it is often difficult to identify the presence of target substructure resonances. This is especially true when the aspect angle of the target causes the temporal overlapping of substructure returns from distinctly different parts of the target structure. To provide a simpler, more easily understood example, the scattered field response of a 1:72 scale B-52 aircraft model to a field incident normal to, and polarized along, the aircraft fuselage was measured in the band 0–18 GHz, and transformed into the time domain [6]. This frequency band provides an equivalent pulse width of about $T_w = 0.04$ ns. The resulting waveform, shown at the bottom of Fig. 1, displays distinct specular events associated with reflections from the main wingtip, the engines, the tail fin, and

Manuscript received September 30, 1997; revised March 27, 1998.

The authors are with the Department of Electrical Engineering, Michigan State University, East Lansing, MI 48824 USA.

Publisher Item Identifier S 0018-926X(98)06883-5.

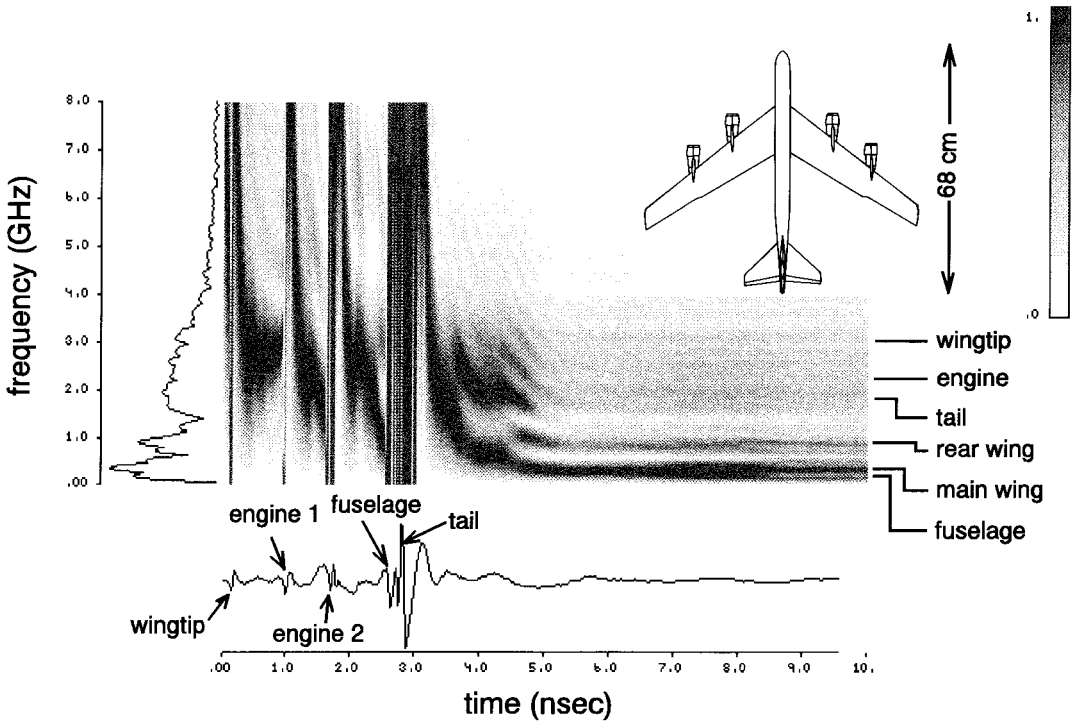

Fig. 1. T-F plot of scale model B-52 aircraft.

the fuselage. The latter portions of the response are dominated by the slowly varying global resonances of the airplane. (Note that there are no specular reflections from structures on the side of the aircraft shadowed by the fuselage.) Each of the first few specular reflections are separated sufficiently in time to observe what appears to be the beginning of substructure resonances. However, it is difficult to visualize these resonances solely from the time domain response; a T-F analysis can provide a more informative picture.

III. An Adaptive-Window-Width STFT for Visualizing Substructure Resonances

A time-frequency plot is often created by sliding a window though the time-domain data and computing the Fourier transform of the data within the window. The choice of the window width determines whether specular or resonant information will be emphasized. A narrow window will isolate specular reflections but will not be wide enough to accommodate the slowly-varying global resonances; a wide window cannot temporally separate resonance and specular information. This problem can be overcome somewhat by using the multiresolutional capabilities of wavelet transforms [2], wherein a "mother" wavelet is expanded and contracted in time as it slides through the data. However, the standard wavelet analysis has no phenomenological basis, and cannot isolate temporal regions where distinct events occur.

To provide a means of isolating and examining the substructure resonances while still providing for a visualization of global resonances, a simple adaptive-window-width STFT algorithm has been devised. The algorithm begins with a window of width T_w. The left edge of the window is fixed in placed, and the right edge is expanded out in time until it encounters a specular reflection. At that point, the left edge is brought forward to again create a window of width T_w. The right edge is then allowed to expand out again, encompassing any resonances generated by the interaction of the incident wave and a target substructure. When the leading edge of the window detects another specular reflection, the left edge of the window is again brought forward to create a window of width T_w and the process repeats. At the point where the final specular reflection is encountered, the window will expand through the late-time period until it reaches the end of the response, enveloping any global resonances which might have been excited.

The above process works well to isolate individual subresonances as long as they are separated sufficiently in time. Obviously, if the subresonance has not had enough time to become established before the onset of another wavefront interaction, visualization of the subresonance will be difficult. Similarly, if substructure resonances from different portions of the target overlap temporally, it will be difficult to identify which spatial event to associate each resonance with. However, that difficulty is not limited to the F-T technique of this letter.

Detection of the substructure specular reflections is problematic. Attempts made to use the shape of the specular reflections (assuming that they are reproductions of the incident pulse) proved no better than those using a simple slope detector. This is probably due to the pulse distortion caused by frequency-dependent diffraction from local structures. The effects of various window shapes were also investigated, with a simple rectangular window found to be most effective. The relatively strong sidelobes were found to be an effective trade-off for the increased frequency localization.

IV. Example

Fig. 1 shows the T-F plot resulting from the algorithm discussed above. Each time point indicates the position of the right side of the moving window. The frequency domain graph to the left of the figure corresponds to the right-most time point. To emphasize the presence of small specular reflections, the Fourier transform corresponding to each time point has been normalized to a maximum magnitude value of unity. Thus, the small reflections from the engines display a strength comparable to the much larger reflection from the fuselage. A linear scale then produces an easy to interpret display.

The first specular reflection occurs from the wingtip, and a developing resonance is easily seen, centered on a 3-GHz resonance frequency. Using a very simple resonance interpretation—that a half wavelength standing wave will span the breadth of a resonant object—3 GHz matches the anticipated resonance of a 5-cm wide wingtip. Similarly, the external resonances building after the reflections from the engines match well with the 2.3-GHz expected resonance frequency for a 6.5-cm-long object (length from front of engine to wing attachment point). Note that there is no internal engine cavity in the models used. Finally, after the incident pulse has interacted with the fuselage and the tail fin, a tail resonance is seen centered at 1.8 GHz, and building global resonances dominated by the fuselage length (0.22 GHz for 68 cm), the main wing length (0.35 GHz for 43 cm), and the rear wing length (1.0 GHz for 15 cm) can be easily seen.

V. Conclusions

An adaptive-window-width short-time Fourier transform provides an effective means for displaying the complicated nature of the transient response of a radar target. An example using the response of a scale model B-52 aircraft shows that the technique is able to isolate individual substructure resonances, while still displaying information about the positions of specular reflections and the existence of long-duration global resonances.

References

[1] Gerhard A. Thielcke, *Bird Sounds.* Ann Arbor, MI: Univ. Michigan Press, 1976.

[2] H. Ling and H. Kim, "Wavelet analysis of backscattering data from an open-ended waveguide cavity," *IEEE Microwave Guided Wave Lett.*, vol. 2, pp. 140–142, Apr. 1992.

[3] A. Moghaddar and E. K. Walton, "Time-frequency distribution analysis of scattering from waveguide cavities," *IEEE Trans. Antennas Propagat.*, vol. 41, pp. 677–680, May 1993.

[4] L. Carin, L. B. Felsen, D. Kralj, S. U. Pillai, and W. C. Lee, "Dispersive modes in the time domain: analysis and time-frequency representation," *IEEE Microwave Guided Wave Lett.*, vol. 4, pp. 23–25, Jan. 1994.

[5] L. Carin and L. B. Felsen, "Wave-oriented data processing for frequency- and time-domain scattering by nonuniform truncated arrays," *IEEE Antennas Propagat. Mag.*, vol. 36, pp. 29–43, June 1944.

[6] E. Rothwell, K. M. Chen, D. P. Nyquist, J. Ross, and R. Bebermeyer, "Measurement and processing of scattered ultra-wideband/short-pulse signals," in *Proc. SPIE Conf. Radar/Ladar Processing Applicat.*, San Diego, CA, July 1995.

Chiral Slab Polarization Transformer for Aperture Antennas

Ari J. Viitanen and Ismo V. Lindell

***Abstract*— The cross polarization of large aperture antennas can be eliminated by a chiral slab transformer in front of the aperture to obtain a more efficient field pattern. The inhomogeneous chirality distribution required can easily be achieved by using a mixture of right- and left-hand helices so that the total density of helices is constant inside the slab. Reflection from the slab can be eliminated by a proper design.**

***Index Terms*—Aperture antennas, inhomogeneous chiral medium, polarization correction.**

I. Introduction

The polarization correction of lens antennas with chiral inclusions was proposed in [1]–[3]. In practice the inhomogeneous chirality distribution inside the lens antennas may be difficult to realize. For practical applications the polarization correction can be easily achieved with a chiral slab in front of a reflector or lens antenna. The required inhomogeneous chiral distribution can be realized by a distribution of chiral inclusions (helices) with opposite handedness. The polarization correction effect is based on the rotation of the polarization plane of the propagating plane wave. The rotation angle is proportional to the chirality parameter κ, which is related to the difference of the refraction index for right-hand and left-hand circularly polarized eigenwaves. The difference of these refraction indices depends on the volume fraction of right-hand helices to left-hand helices in chiral matrix. In the structure analyzed here[1] the total number of helices per volume is held constant but the ratio of the number of right-hand helices versus left-hand helices is changing which gives us as a result an inhomogeneous chirality parameter. Because the total density of helices is constant throughout the slab, the wave impedance inside the slab is constant. This is because the medium parameters μ and ϵ are not affected by the handedness of the inclusions. As an example, it is demonstrated that the cross polarization of the field from a dipole source at the focus of a parabolic reflector antenna can be eliminated with a chiral slab located at the aperture of the antenna.

II. Theory

Let us consider reflection and transmission of fields through a chiral slab $0 < z < d$. On the aperture plane ($z < 0$) the incident and reflected electric fields are $\mathbf{E}_1(z) = \mathbf{E}^i e^{-jk_o z} + \mathbf{E}^r e^{jk_o z}$ and the transmitted electric field after the slab, when $z > d$ is $\mathbf{E}_3(z) = \mathbf{E}^t e^{-jk_o z}$. In between there is a chiral slab where the electric field is written as [3]

$$\mathbf{E}_2(z) = E_+ \mathbf{u}_+ e^{-jk_+ z} + E_- \mathbf{u}_- e^{-jk_- z} + E_+^r \mathbf{u}_+^* e^{jk_+ z} + E_-^r \mathbf{u}_-^* e^{jk_- z} \quad (1)$$

where $k_\pm = k_o(n \mp \kappa)$ and $\mathbf{u}_+ = 1/\sqrt{2}(\mathbf{u}_x - j\mathbf{u}_y)$ and $\mathbf{u}_- = 1/\sqrt{2}(\mathbf{u}_x + j\mathbf{u}_y)$ are the right- and left-hand circularly polarized

Manuscript received March 25, 1998.

The authors are with the Electromagnetics Laboratory, Helsinki University of Technology, Helsinki FIN-02015 HUT, Finland.

Publisher Item Identifier S 0018-926X(98)06684-8.

[1] Patent pending FI974 116